

Journal of Biomedical Optics

BiomedicalOptics.SPIEDigitalLibrary.org

Coherent anti-Stokes Raman scattering hyperspectral imaging of cartilage aiming for state discrimination of cell

Manabu Shiozawa
Masataka Shirai
Junko Izumisawa
Maiko Tanabe
Koich Watanabe

SPIE.

Manabu Shiozawa, Masataka Shirai, Junko Izumisawa, Maiko Tanabe, Koich Watanabe, "Coherent anti-Stokes Raman scattering hyperspectral imaging of cartilage aiming for state discrimination of cell," *J. Biomed. Opt.* **21**(7), 076004 (2016), doi: 10.1117/1.JBO.21.7.076004.

Coherent anti-Stokes Raman scattering hyperspectral imaging of cartilage aiming for state discrimination of cell

Manabu Shiozawa,^{a,*} Masataka Shirai,^a Junko Izumisawa,^a Maiko Tanabe,^b and Koich Watanabe^a

^aHitachi, Ltd., Center for Technology Innovation, Research and Development Group, 1-280, Higashi-Koigakubo, Kokubunji, Tokyo 185-8601, Japan

^bHitachi, Ltd., Center for Exploratory Research, Research and Development Group, 1-280, Higashi-Koigakubo, Kokubunji, Tokyo 185-8601, Japan

Abstract. Noninvasive cell analyses are increasingly important in the medical field. A coherent anti-Stokes Raman scattering (CARS) microscope is the noninvasive imaging equipment and enables to obtain images indicating molecular distribution. However, due to low-signal intensity, it is still challenging to obtain images of the fingerprint region, in which many spectrum peaks correspond to compositions of a cell. Here, to identify cell differentiation by using multiplex CARS, we investigated hyperspectral imaging of the fingerprint region of living cells. To perform multiplex CARS, we used a prototype of a compact light source generating both pump light and broadband Stokes light. Assuming application to regenerative medicine, we chose a cartilage cell, whose differentiation is difficult to be identified by change of the cell morphology. Because one of the major components of cartilage is collagen, we focused on distribution of proline, which accounts for approximately 20% of collagen. The spectrum quality was improved by optical adjustments of the power branching ratio and divergence of Stokes light. Periphery of a cartilage cell was highlighted in a CARS image of proline, and this result suggests correspondence with collagen generated as an extracellular matrix. The possibility of noninvasive analyses by using CARS hyperspectral imaging was indicated. © 2016 Society of Photo-Optical Instrumentation Engineers (SPIE) [DOI: [10.1117/1.JBO.21.7.076004](https://doi.org/10.1117/1.JBO.21.7.076004)]

Keywords: coherent anti-Stokes Raman scattering; multiplex coherent anti-Stokes Raman scattering; hyperspectral imaging; super-continuum light; cartilage; proline.

Paper 160199PRR received Mar. 29, 2016; accepted for publication Jun. 17, 2016; published online Jul. 8, 2016.

1 Introduction

Cell analyses are increasingly important in medical fields such as regenerative medicine and drug development. A microscope using reagent for staining is widely used for cell analyses. However, due to invasive diagnostics, it is difficult to analyze the same cell continuously and to implant stained cells into patients. A Raman microscope is one of the noninvasive equipment and can identify molecular species. Although several studies on state discriminations of cells by using Raman spectrum have been reported,¹⁻³ due to low-signal intensity, there have been few reports in which Raman images have been obtained. Second-harmonic generation is a means to obtain images of molecular distribution noninvasively;^{4,5} however, only molecules without symmetry can be imaged. Coherent anti-Stokes Raman scattering (CARS) was proposed by Duncan et al.,⁶ and various systems have been developed in more recent years.⁶⁻¹² Multiplex CARS is one of the promising ways to obtain the Raman signal of a fingerprint region (800 to 1800 cm^{-1}), in which there are many spectrum peaks corresponding to compositions of a cell, simultaneously.¹³⁻¹⁵ Although the CARS microscope can have signal intensity orders of magnitude higher than a Raman microscope, the CARS imaging of a fingerprint region is still challenging.

In this report, we investigated hyperspectral imaging of cartilage cells by multiplex CARS to identify the differentiation state. Although a variety of short pulse lasers which can emit light on the order of watt is provided recently and quality of CARS spectrum can be improved readily, we investigated optical adjustment using a compact microchip laser in consideration of the practical use and damage to cells. The effect of the optical adjustment was demonstrated to improve quality of CARS spectrum and to obtain images of a fingerprint region. Periphery of a cartilage cell was highlighted in a CARS image of proline, and this result suggests correspondence with collagen generated as an extracellular matrix. These results indicated the possibility of cell analyses by using CARS hyperspectral imaging.

2 Methods

2.1 Experimental Setup

A schematic of a CARS experimental setup is shown in Fig. 1. The prototype module of a laser light source, which can generate both pump and broadband Stokes lights by using a photonic crystal fiber (PCF), was used to perform multiplex CARS.¹⁶ Pulse duration, center wavelength, average power, and repetition rate of the microchip laser (Horus laser HLX-I-F040) used in the module were 1.1 ns, 1064 nm, 495 mW, and 27 kHz. The laser light was branched to PCF (NKT Photonics SC-5.0-1040-PM) and single-mode fiber (Nufem PM980-XP)

*Address all correspondence to: Manabu Shiozawa, E-mail: manabu.shiozawa.ar@hitachi.com

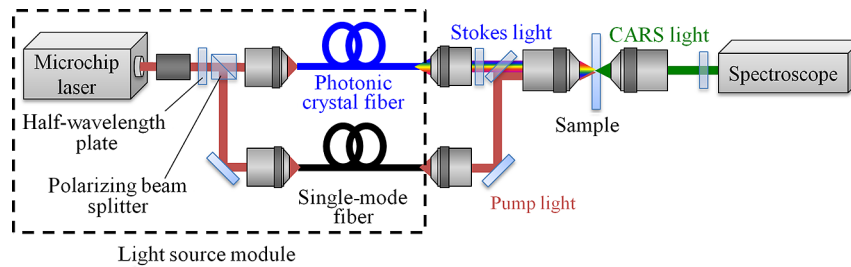


Fig. 1 Schematic of experimental setup for multiplex CARS.

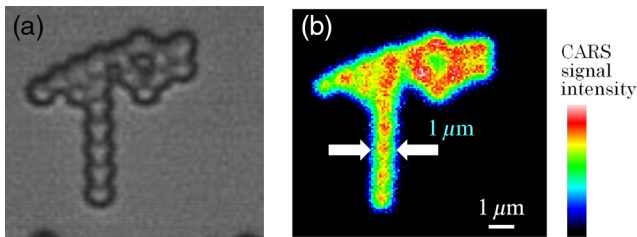


Fig. 2 (a) Bright-field image and (b) CARS image of 1- μm polystyrene beads.

by using a half-wavelength plate and polarizing beam splitter. The pump and Stokes lights were combined by a dichroic mirror and focused into a sample by an objective lens (Nikon CFI Apo LWD 40xWI, NA 1.15). When pump and Stokes lights are focused at the same position in a sample, CARS light is generated. Average powers of pump and Stokes lights measured after passing through the objective were approximately 50 and 10 mW, respectively. CARS spectrum was obtained by a spectroscope (Princeton PIXIS400, Acton SP-2358), and Raman spectrum was reconstructed by the maximum entropy method (MEM).¹⁷ After the reconstruction, the quality of spectra was improved by singular value decomposition (SVD).¹⁸ It is one of the advantages of multiplex CARS to be able to use SVD comparing with monochromatic CARS. To adjust power ratio between pump and Stokes lights, a half-wavelength plate was rotated. Divergence of Stokes light was adjusted by changing position of a collimator lens for PCF to adjust multiplexing condition of pump and Stokes lights.

CARS images were obtained by changing position of a sample by using a piezo stage. The typical size of CARS image and acquisition time to obtain the image were $50 \times 50 \mu\text{m}^2$ and 5 min, respectively. Figure 2 shows a CARS image indicating distribution of CH_2 stretch (2900 cm^{-1}) in 1- μm polystyrene beads. The lateral resolution was estimated at approximately $1 \mu\text{m}$ from measured width of the beads.

2.2 Sample

Assuming application to regenerative medicine, cartilage cells differentiated by the following method were measured as a sample. Approximately 4×10^4 C3H10T1/2 cells were seeded onto a 35-mm ϕ glass-bottom dish and incubated in 2-mL D-MEM (Dulbecco's Modified Eagle Medium) D6429 under 5% CO_2 at 37°C for 2 days. To induce differentiation, the medium was replaced with 2 mL of the D-MEM containing 100 ng/mL bone morphogenetic protein 2 (BMP-2) in another 2 days. For comparison, the medium was just changed to a new D-MEM in a control sample. After culturing for 3 days, the cell density was adjusted to 1×10^4 to obtain CARS images as a single cell.

Figures 3(a) and 3(b) show typical bright-field images of the cells cultured with and without BMP-2, respectively. It is difficult to identify differentiation by cell morphology, so cell composition needs to be analyzed. Because one of the major components of cartilage is collagen, we focused on distribution of proline, which generally accounts for approximately 20% of collagen. Spectra of gelatin and adipose cell were compared with confirm signal of proline because gelatin is extracted from collagen and was expected to show greater signal than adipose. Adipose cells were also used to measure the effect of optical adjustment because adipose shows several spectrum peaks in fingerprint region and is suitable to investigate signal-to-noise ratio (SNR) of spectrum. To validate a CARS image of proline, the stained image by using sirius red F3B of the same cell was obtained after CARS measurement.

3 Results and Discussion

3.1 Optical Adjustment to Obtain CARS Images of Fingerprint Region

To obtain CARS images of weak spectrum peak in a fingerprint region such as proline, an optical adjustment method was investigated. Because CARS is a third-order nonlinear optical effect, adjustment of the power ratio between pump and Stokes lights is

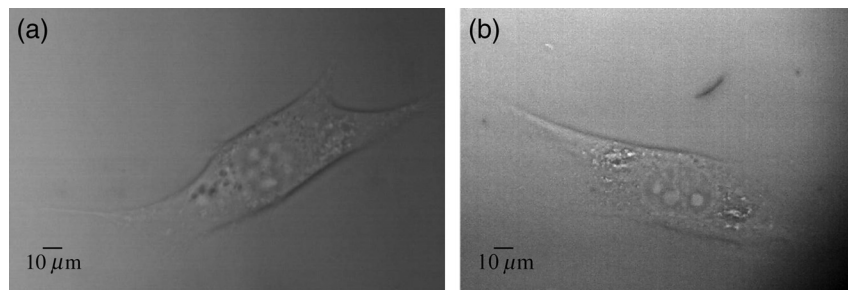


Fig. 3 Typical bright-field images of the cell cultured (a) with and (b) without BMP-2.

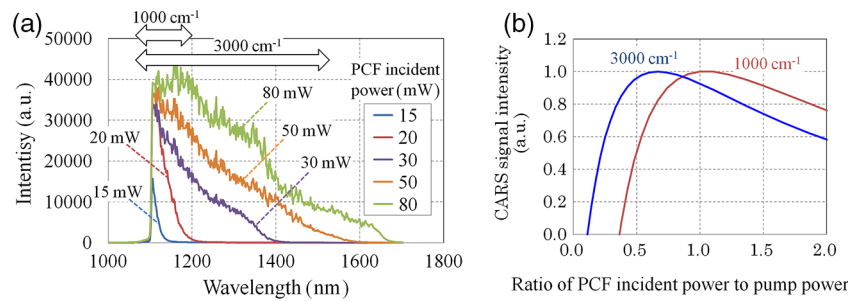


Fig. 4 (a) Stokes light spectra depending on PCF incident laser power. (b) Relationship between CARS signal intensity and power branching ratio of incident light on PCF to that on single-mode fiber to propagate pump light.

essential, especially under the condition with limited laser power. Figure 4(a) shows the spectra of broadband Stokes light generated by PCF. The spectrum changed depending on incident laser power, and it is needed to exceed a threshold power to generate Stokes light with a specific wavelength. For example, to generate Stokes light with a wavelength of 1550 nm, which contributes to the generation of CARS light with approximately 3000 cm^{-1} , the incident laser power higher than 50 mW is necessary. On the other hand, the threshold is 20 mW to generate Stokes light with 1200 nm, and the rest of the laser power could be used as pump light. CARS light power is proportional to Stokes light power and the square of pump light power, so the signal intensity can be calculated by using the generation characteristic of broadband Stokes light. Figure 4(b) shows the relationship between power branching ratio and CARS signal intensity calculated by the following equation:

$$I_{\text{CARS}} = \left(\frac{1}{\alpha + 1} I_{\text{total}} \eta_{\text{pump}} \right)^2 \left(\frac{\alpha}{\alpha + 1} I_{\text{total}} - I_{\text{th}} \right) \eta_{\text{PCF}} \eta_{\text{Stokes}}, \quad (1)$$

where α is the power branching ratio, I_{total} is the laser power before branching, I_{th} is the threshold power, and η_{PCF} is the generation efficiency of Stokes light using PCF, while η_{pump} and η_{Stokes} represent the optical efficiency of pump and Stokes lights in a setup, respectively. Figure 4(b) indicates that the power branching ratio should be adjusted depending on the target wavelength of CARS light.

Furthermore, intensity of CARS signal is highly sensitive to the multiplexing condition of pump and Stokes lights. When Stokes light is focused in a measurement sample by an objective lens, chromatic aberration occurs due to broadband characteristics and focal point differs slightly depending on the wavelength. Because CARS light is generated at only region where both pump and Stokes lights are focused, the shape of the CARS spectrum changes depending on multiplexing condition of pump and Stokes lights.

Figure 5(a) shows the CARS spectra at the same position of adipose by changing optical adjustments described previously. A strong peak of C—H stretch at 2900 cm^{-1} was obtained; however, intensities of peaks in the fingerprint region were extremely weak before the adjustment. On the other hand, although the peak of C—H stretch disappeared, peaks in the fingerprint region improved after the adjustment. The SNR of peaks in fingerprint region is compared in Fig. 5(b). We defined signal as the difference between top and bottom levels of the peak. Noise was defined as the average intensity of high-frequency component, which corresponds to fluctuation at less than approximately 5 cm^{-1} , after fast Fourier transformation of the spectrum. The SNR was confirmed to improve by more than 5 dB. The SNR of low wavenumber peaks such as amide III was improved greater than high wavenumber signal by the adjustment targeting at lower wavenumbers.

3.2 CARS Hyperspectral Imaging of Cartilage

To confirm signal of proline, a spectrum of gelatin was investigated prior to measurement of a cartilage cell. Figure 6

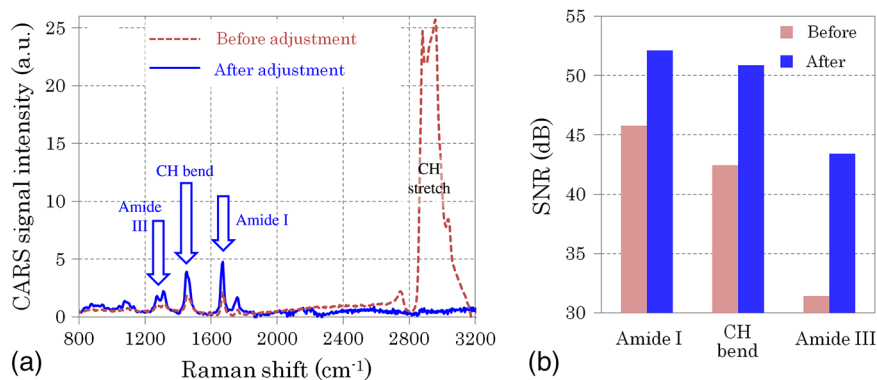


Fig. 5 (a) CARS spectra measured at the same position of adipose by changing optical adjustment. (b) SNR comparison before and after optical adjustment.

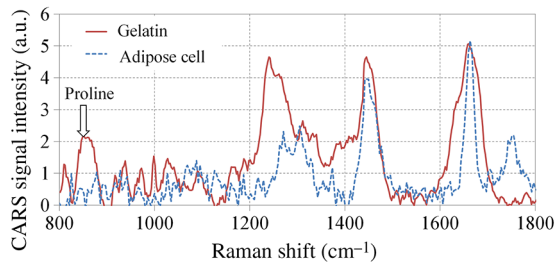


Fig. 6 Spectrum comparison between gelatin and adipose cell.

compares the spectra of gelatin and an adipose cell. The spectrum peak of proline¹ was obtained at approximately 860 cm⁻¹. Figures 7(a) and 7(b) show a bright-field image and CARS spectra at points A and B of a cartilage cell, respectively. Several spectrum peaks containing proline were obtained at point A (region of cell). CARS images of amide I (~1650 cm⁻¹), phenylalanine (~1000 cm⁻¹), and proline (~860 cm⁻¹) are shown in Figs. 8(a), 8(b), and 8(c), respectively. CARS hyperspectral images were successfully obtained by the optical adjustment described above. Images of amide I and phenylalanine

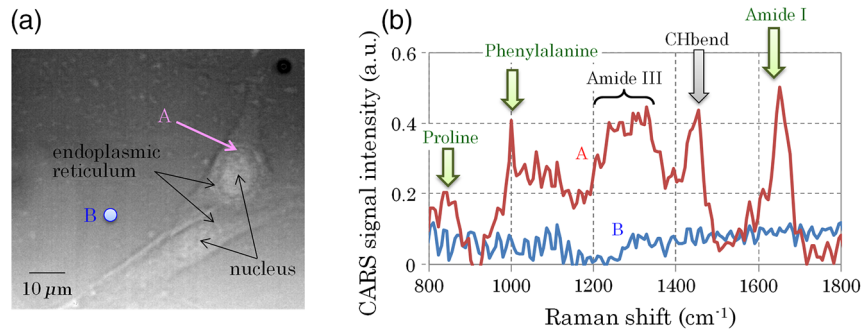


Fig. 7 (a) Bright-field image of cartilage cells. (b) CARS spectra at points A and B.

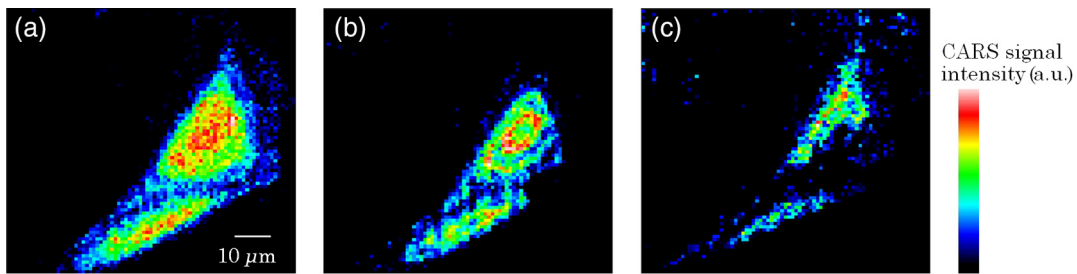


Fig. 8 CARS images of (a) amide I, (b) phenylalanine, and (c) proline.

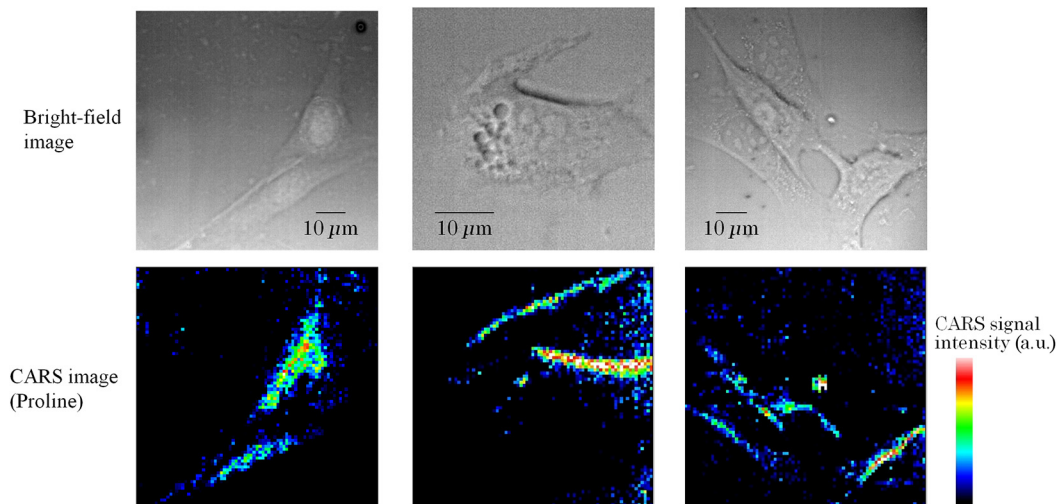


Fig. 9 Correspondences of bright-field image and CARS image of proline.

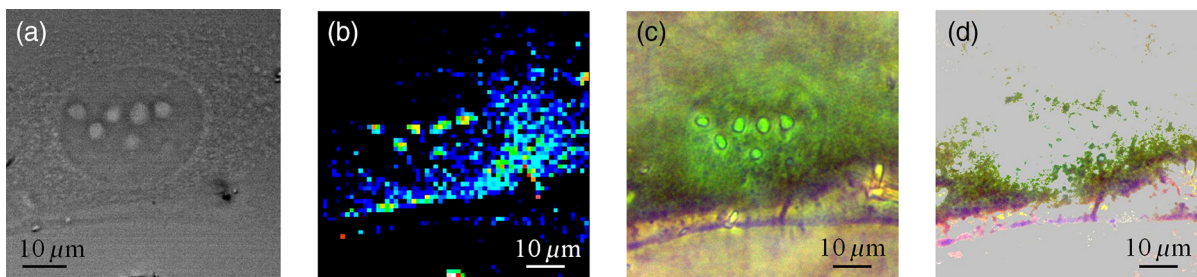


Fig. 10 (a) Bright-field image, (b) CARS image, (c) stained image, and (d) extraction image of region containing purple of cartilage cell.

indicate that those molecules were distributed throughout the cell. On the other hand, periphery of the cell is highlighted in the CARS image of proline. Figure 9 shows the bright-field images and CARS images of proline of other cells. Periphery of the cell was confirmed to be highlighted in each CARS image.

Figure 10 shows the comparison of CARS image of proline and the stained image. Periphery of the cell was highlighted in Fig. 10(b) as discussed previously. Figure 10(c) is the stained image of the same cell by using Sirius Red F3B. Collagen and other protein were stained green and purple, respectively. The extraction image of the region containing purple by image processing of Fig. 10(c) is shown in Fig. 10(d). Comparing Figs. 10(b) and 10(d), periphery of the cell is emphasized in both images. These results suggest that the CARS image of proline shows a distribution of generated collagen, an extracellular matrix. Because cells were seeded as a single cell, collagen would be localized at a portion of the cell periphery.

4 Conclusion

The hyperspectral imaging of cartilage cells by multiplex CARS was investigated. The SNR of CARS spectrum was improved by optical adjustment for power branching ratio and divergence of broadband Stokes light. Hyperspectral images were successfully obtained by improving SNR. Periphery of a cartilage cell was highlighted in the CARS image of proline, and this result suggests correspondence with collagen generated as an extracellular matrix. The possibility of cell analyses by using CARS hyperspectral imaging was indicated. For practical use, implementation of adjustment system, such as a collimator lens for PCF and adjustment sequence, would be challenging because highly accurate adjustment on the order of micrometer is required.

Acknowledgments

We thank Professor Ung-il Chung and Dr. Hironori Hojo for offering C3H10T1/2 cells.

References

1. N. S. J. Lim et al., "Early detection of biomolecular changes in disrupted porcine cartilage using polarized Raman spectroscopy," *J. Biomed. Opt.* **16**(1), 017003 (2011).
2. A. Kunstar et al., "Label-free Raman monitoring of extracellular matrix formation in three-dimensional polymeric scaffolds," *J. R. Soc., Interface* **10**(86), 20130464 (2013).
3. A. Kunstar et al., "Recognizing different tissues in human fetal femur cartilage by label-free Raman microspectroscopy," *J. Biomed. Opt.* **17**(11), 116012 (2012).
4. T. Yasui et al., "In vivo observation of age-related structural changes of dermal collagen in human facial skin using collagen-sensitive second harmonic generation microscope equipped with 1250-nm mode-locked Cr:Forsterite laser," *J. Biomed. Opt.* **18**(3), 031108 (2012).
5. P. P. Provenzano et al., "Collagen density promotes mammary tumor initiation and progression," *BMC Med.* **6**(1), 11 (2008).
6. M. D. Duncan et al., "Scanning coherent anti-Stokes Raman microscope," *Opt. Lett.* **7**(8), 350–352 (1982).
7. A. Zumbusch et al., "Three-dimensional vibrational imaging by coherent anti-Stokes Raman scattering," *Phys. Rev. Lett.* **82**(20), 4142–4145 (1999).
8. J. X. Cheng and X. S. Xie, "Coherent anti-Stokes Raman scattering microscopy: instrumentation, theory, and applications," *J. Phys. Chem. B* **108**(27), 827–840 (2004).
9. A. Volkmer et al., "Vibrational imaging with high sensitivity via epide- tected coherent anti-Stokes Raman scattering microscopy," *Phys. Rev. Lett.* **87**(2), 023901 (2001).
10. J.-X. Cheng et al., "Polarization coherent anti-Stokes Raman scattering microscopy," *Opt. Lett.* **26**(17), 1341–1343 (2001).
11. L. Y. Jong et al., "Optimized continuum from a photonic crystal fiber for broadband time-resolved coherent anti-Stokes Raman scattering," *Opt. Express* **18**(5), 4371–4379 (2010).
12. A. Volkmer et al., "Time-resolved coherent anti-Stokes Raman scattering microscopy: imaging based on Raman free induction decay," *Appl. Phys. Lett.* **80**(9), 1505–1507 (2002).
13. J. P. R. Day et al., "Quantitative coherent anti-Stokes Raman scattering (CARS) microscopy," *J. Phys. Chem. B* **115**(24), 7713–7725 (2011).
14. M. Okuno et al., "Ultrabroadband multiplex CARS microspectroscopy and imaging using a subnanosecond supercontinuum light source in the deep near infrared," *Opt. Lett.* **33**(9), 923–925 (2008).
15. C. H. Camp, Jr. et al., "High-speed coherent Raman fingerprint imaging of biological tissues," *Nat. Photonics* **8**(8), 627–634 (2014).
16. H. Mikami et al., "Compact light source for ultrabroadband coherent anti-Stokes Raman scattering (CARS) microscopy," *Opt. Express* **23**(3), 2872–2878 (2015).
17. E. M. Vartiainen et al., "Direct extraction of Raman line-shapes from congested CARS spectra," *Opt. Express* **14**(8), 3622–3630 (2006).
18. K. Alexander et al., "Hyperspectral imaging and characterization of live cells by broadband coherent anti-Stokes Raman scattering (CARS) microscopy with singular value decomposition (SVD) analysis," *Appl. Spectrosc.* **68**(10), 1116–1122 (2014).

Manabu Shiozawa received his MS degree in engineering from Nagoya University in 2003. He then joined Hitachi Ltd., where he has been engaged in development of reading and writing techniques for optical storage systems. He is currently the team leader of the CARS development team in the R&D group.

Biographies for the other authors are not available.